



Review

Pectin-silica gels as matrices for controlled drug release in gastrointestinal tract



Fedor V. Vityazev^{a,*}, Maiia I. Fedyuneva^a, Victoria V. Golovchenko^a, Olga A. Patova^a, Elena U. Ipatova^b, Eugene A. Durnev^c, Ekaterina A. Martinson^c, Sergey G. Litvinets^c

^a Institute of Physiology, Komi Science Centre, The Urals Branch of the Russian Academy of Sciences, 50, Pervomaiskaya Str., 167982 Syktyvkar, Russia

^b Institute of Chemistry, Komi Science Centre, The Urals Branch of the Russian Academy of Sciences, 48, Pervomaiskaya Str., 167982 Syktyvkar, Russia

^c Federal Government-Financed Educational Institution of Higher Professional Education «Vyatka State University», 36, Moskovskaya Str., 610000, Kirov, Russia

ARTICLE INFO

Article history:

Received 6 May 2016

Received in revised form

12 September 2016

Accepted 15 September 2016

Available online 16 September 2016

Chemical compounds studied in this article:

Tetraethoxysilane (PubChem CID: 6517)

Ethanol (PubChem CID: 702)

Hydrochloric acid (PubChem CID: 313)

Sodium metasilicate (PubChem CID: 23266)

Sodium chloride (PubChem CID: 5234)

Potassium dihydrogen phosphate

(PubChem CID: 516951)

Calcium chloride (PubChem CID: 5284359)

5-Aminosalicylic acid (PubChem CID: 4075)

Keywords:

Pectin-silica beads

FTIR spectra

Texture analysis

Controlled release

Mesalazine

ABSTRACT

The synthesis of pectin-silica gels for controlled drug release in gastrointestinal tract (GIT) using low methoxyl (LM) and high methoxy (HM) pectins and tetraethoxysilane (TEOS) as precursor is described. The FTIR spectra of the pectin-silica gels show intense absorption bands at 1246 cm⁻¹ and 802 cm⁻¹ corresponding to the vibrations —C—O—Si— bonds, which absent in the FTIR spectra of the native pectins that indicate the formation covalent bond between silica and pectin macromolecules in the pectin-silica gels. Pectin-TEOS, pectin-Ca-TEOS and pectin-TEOS-Ca beads with mesalazine are synthesized by different combinations of sol-gel method using TEOS and ionotropic gelation method using calcium chloride. The best resistant of pectin-TEOS and pectin-Ca-TEOS beads during incubation in simulated gastric fluid for 2 h and subsequently in simulated intestinal fluids for 18 h is indicated. Pectin-TEOS beads are characterized by higher encapsulation efficiency (to 28%) than pectin-Ca-TEOS beads (to 16%). The drug release of pectin-silica beads in simulated GIT occurs gradually up to 80% and is directly dependent on the hardness of the beads. The surface morphology of beads is shown. The use of pectin-silica beads is promising with regard to the development of controlled release of drug formulations.

© 2016 Elsevier Ltd. All rights reserved.

Contents

1. Introduction.....	10
2. Materials and methods.....	10
2.1. Materials.....	10
2.2. General analytical methods.....	10
2.3. Preparation of pectin-silica gels.....	11
2.3.1. Preparation of pectin-silica plates.....	11
2.3.2. Preparation of pectin-silica beads.....	11
2.3.3. Preparation of mesalazine loaded pectin-silica beads.....	11
2.4. Texture analyses of pectin-silica gels.....	11

* Corresponding author.

E-mail address: rodefex@mail.ru (F.V. Vityazev).

2.5.	Study of size and morphology of gel beads	11
2.6.	Water holding capacity	11
2.7.	Drug loading and encapsulation efficiency	11
2.8.	Evaluation of the stability of beads in an environment simulating the GIT	12
2.9.	Mesalazine release <i>in vitro</i>	12
3.	Results and discussion	12
3.1.	Formation of pectin-silica gels	12
3.2.	Infrared spectroscopy pectin-silica gels	12
3.3.	Structural and mechanical properties of pectin-silica gels	15
3.4.	Morphological analysis of the beads by SEM	16
3.5.	Stability of the beads in an environment simulating the GIT	17
3.6.	Estimation of the mesalazine loading and the encapsulation efficiency of the beads	18
3.7.	<i>In vitro</i> mesalazine release from the beads	18
4.	Conclusions	18
	Acknowledgement	19
	References	19

1. Introduction

Ulcerative colitis is the one of the most severe diseases of the digestive system. Prevalence of the disease is increasing with time and in different regions around the world (Latella & Papi, 2012; Ouyang et al., 2005). According to the epidemiological studies, the total number of patients with ulcerative colitis is from 25 to 240 per 100 thousand. The mortality rate ranges from 0.4 to 0.7 per 100 thousand populations per year (Kappelman et al., 2008; Kornbluth & Sachar, 2010; Munkholm, 2003; Satyrova & Mikhailova, 2010). An increasing number of diseases, attaches social importance to problem of medical treatment of ulcerative colitis. The disease has a significant impact on the quality of life for the majority of patients (Boonen et al., 2002). Patients with ulcerative colitis often require hospitalization, specialized medical care and regular intake of medicines (Longobardi, Jacobs, & Bernstein, 2004). Nowadays, the main drugs in the treatment of ulcerative colitis are the products based on the 5-amino salicylic acid (mesalazine) (Desreumaux & Ghosh 2006; Iacucci, de Silva, & Ghosh, 2010). The major limitation for its oral administration is the instability under the stomach conditions and rapidly metabolized and inactivated in the intestinal mucosa, becoming inactive *N*-acetyl-5-aminosalicylic acid, which leads to low efficiency and other serious side effects (Desreumaux & Ghosh, 2006; Schroeder, 2002). Effects from mesalazine are dose-dependent, so it is important to ensure necessary concentrations of mesalazine in the field of inflammation. Therefore, the creation of effective coatings, which will prevent unwanted loss of mesalazine in the unaffected areas of the gastrointestinal tract (GIT) and thus ensure maximum delivery to the colon, is an urgent task.

The creation of hybrid materials consisting of biopolymers and inorganic complexing agent develops rapidly nowadays. Organosilicon compounds occupy a special place among the hybrid materials. It is shown that porous silicon-based materials can biodegrade in the gastric environment, and silicone is a suitable material for the encapsulation, transmission and effective release of drugs (Salonen, Kaukonen, Hirvonen, & Lehto, 2008; Vivero-Escoto, Slowing, Trewyn, & Lin, 2010). In the preparation of organosilicon compounds in particular polysaccharide-silica compounds, different precursors such as tetraethyl orthosilicate (TEOS) (Angelova, Rangelova, Yuryev, Georgieva, & Muller, 2012; Assifaoui, Bouyer, Chambin, & Cayot, 2013; Rangelova, Aleksandrov, Angelova, Georgieva, & Muller, 2014; Samuneva et al., 2008), sodium metasilicate (Nurdin & Purwasasmita, 2013; Wu et al., 2011) and tetrakis (2-hydroxyethyl) orthosilicate (Shchipunov & Karpenko, 2004) are used. One of the most desirable biopolymers for the preparation of protective coatings is pectin. Pectin demonstrates diverse physiological activities: immunomodulatory, antidotal, antioxidant, gastroprotective (Khasina, Sgrebneva, Ovodova, Golovchenko, &

Ovodov, 2003; Popov, Popova, Nikolaeva, Golovchenko, & Ovodova, 2005; Popov et al., 2013; Popov et al., 2014). It is known that pectic polysaccharides form stable gels (Capel, Nicolai, Durand, Boulenger, & Langendorff, 2006; Patova, Golovchenko, & Ovodov, 2014; Ventura, Jammal, & Bianco-Peled, 2013), due to the low toxicity, are promising materials for the creation of protective materials for drug delivery on their basis. It is shown that pectin can be used as a protective sheath for delivery of biologically active ingredients or drugs (Das, Ng, & Ho, 2011; Kawadkar, Chauhan Meenakshi, & Ram, 2010; Mohanty & Anigrahi, 2015; Sriamornsak, 2011). Purpose of this work is to produce a matrix based on silica and pectin for the immobilization of drugs (mesalazine).

2. Materials and methods

2.1. Materials

Apple pectins AU701 and AU202 (Herbstreith & Fox, Germany). Chemical reagents: tetraethoxysilane (TEOS) (Fluka, France), ethanol (95%, JSC Kirov Pharmaceutical Factory, Russia), hydrochloric acid (Neva Reaktiv, Russia), sodium chloride (Neva Reaktiv, Russia), potassium dihydrogen phosphate (Neva Reaktiv, Russia), calcium chloride (99%, Sigma-Aldrich, Germany) and mesalazine (Aldrich, China).

2.2. General analytical methods

The uronic acid content was determined by the reaction with 3,5-dimethylphenol in the presence of concentrated sulfuric acid and a calibration plot was constructed for D-galacturonic acid; photocolourimetry was carried out at the following two wavelengths: 400 and 450 nm (Usov, Bilan, & Klochkova, 1995). The amount of methoxyl groups was determined by a previously described method (Wood & Siddiqui, 1971) and from the calibration plot constructed for methanol; photocolourimetry was carried out at 412 nm. Spectrophotometric measurements were made with an Ultrospec 3000 spectrophotometer (England). Pectin average molar masses were determined using HP-SEC on a chromatographic system (Shimadzu, Japan) by a previously described method (Popov et al., 2014). Qualitative and quantitative determination of neutral monosaccharides in the form of corresponding polyol acetates was carried out using GC in a Varian 450-GC (Netherlands) chromatograph by a previously described method (Popov et al., 2014). FTIR spectra of samples dehydrated in a Fisher pistol in vacuum over P₂O₅ at 60 °C were recorded using a FTIR Prestige-21 (Shimadzu, Japan) spectrophotometer ($\nu_0 = 4000 \text{ cm}^{-1}$, $\nu_K = 400 \text{ cm}^{-1}$, IT = 1). Samples (2 mg) were analyzed as beads obtained by pressing with KBr.

Table 1
Chemical characteristics of pectins.

Pectin	UA ^a	Gal ^a	Xyl ^a	Glc ^a	Rha ^a	Ara ^a	OMe ^a	DM (%) ^b	Mw, kDa	Mw/Mn
AU701	86.5	2.3	2.8	1.5	1.3	0.3	6.2	43	401	5.2
AU202	78.0	6.4	2.4	1.7	1.9	2.0	10.8	82	506	7.6

^a Data were calculated as weight%.^b Degree of methylation.**Table 2**
The formulation composition, physical properties of pectin-silica plates.

Pectin-silica compounds	C (T ₉₀ C), mol/l	Young modulus E, kPa
AU701-1	0.25	15.4 ± 4.5
AU701-2	0.50	42.1 ± 12.1
AU701-3	0.75	77.1 ± 11.4
AU701-4	1.00	109.9 ± 23.8
AU202-1	0.25	n.d.
AU202-2	0.50	n.d.
AU202-3	0.75	26.6 ± 4.1
AU202-4	1.00	47.2 ± 8.6

n.d.—not identified.

2.3. Preparation of pectin-silica gels

2.3.1. Preparation of pectin-silica plates

The pectin solution (AU701, AU202), TEOS (0.25 M, 0.50 M, 0.75 M and 1.00 M) (4 mL) were placed in Petri plate (d = 3.4 cm) and HCl (0.01 mL) was added under continuous stirring and then the reaction mixture was incubated for 24 h (after adding of the end components the pectin concentration was 2%). After 24 h the released liquid was removed from the gel surface. The obtained plate was washed 2–3 times with distilled water to neutral pH and lyophilized (VirTis FREEZEMOBILE 3+SL, USE).

2.3.2. Preparation of pectin-silica beads

Pectin (AU701) was dissolved in dist. water up to a concentration 20 mg/mL (2%). Pectin solution was extruded drop-wise with a 0.6 mm diameter needle into 50% aqueous ethanol solution containing TEOS (0.25 M, 0.50 M, 0.75 M and 1.00 M) and 0.2 mL of 0.5 M HCl with constant stirring and held for 24 h. After 24 h, the beads were separated on the grid, washed 2–3 times with dist. water to neutral pH. Then the each portion of beads was divided into two equal parts. Further, the first batch was dried out at 25 °C temperature. The second part of obtained beads was placed in a 1.0 M calcium chloride solution for 1 h. Then beads were washed on the grid 2–3 times with dist. water to neutral pH and were dried at 25 °C. These beads were obtained in combination *pectin-TEOS* and *pectin-TEOS-Ca* respectively (Table 3).

Pectin (AU701) was dissolved in dist. water up to a concentration 20 mg/mL (2%). Pectin solution was extruded dropwise with a 0.6 mm diameter needle into 50% aqueous ethanol solution containing calcium chloride (1.0 M) with constant stirring and held for 1 h. After that, obtained beads were washed on the grid, 2–3 times with dist. water to neutral pH and were separated into five portions. The first portion was left unchanged and was dried at 25 °C. The remaining four portions were placed in 50% aqueous ethanol solution containing TEOS (0.25 M, 0.50 M, 0.75 M and 1.00 M), HCl (0.5 M, 0.2 mL) and incubated for 24 h. After 24 h beads were washed on the grid 2–3 with dist. water to neutral pH. Further, the formed beads were dried similarly to the first portion. These beads were obtained in combination *Ca-pectin* and *pectin-Ca-TEOS* respectively (Table 3).

2.3.3. Preparation of mesalazine loaded pectin-silica beads

To a 2% solution of pectin was added mesalazine (drug content is 0.25%, 0.50%, 1.00% and 2.00%). The resulting dispersion was added dropwise to a solution of 50% aqueous ethanol solution containing

TEOS (1.0 M) and HCl (0.5 M, 0.2 mL) or CaCl₂ (1.0 M) under continuous stirring. Further was done similarly as in the preparation of beads with TEOS.

2.4. Texture analyses of pectin-silica gels

A software-controlled dynamometer TA-XT.Plus Texture Analyzer (Stable Micro Systems, UK) with a 5-kg load cell was used for the mechanical characterization of the wet plates (height 4 mm) and the wet beads (height 3 mm). The resistance of hydrogel to penetration and the hardness were obtained with ebonite cylindrical probes (P/0.5R and P/5), diameters are 5.0 mm and 12.7 mm, respectively. The pre- and post-test speed was 10.0 mm/s and the test speed was 0.1 mm/s until a deformation of 50%. Each analysis was executed 25 (on different beads) and 10 (on different plates) times. All calculations of maximum peaks were performed using Texture Exponent 6.1.4.0 software (Stable Micro Systems, UK).

2.5. Study of size and morphology of gel beads

The shape and size of beads were recorded with an optical microscope (Altami, Russia) fitted with a camera and an image analysis system (Altami Studio 3.2, Russia). Each analysis was executed on 25 different beads. Under the same optical conditions, an image of a linear scale was used for calibration. One pixel corresponds to 0.024 mm. Standard error of measurement was 0.012 mm. Aspect ratio (AR) of the beads calculated based on the results of analysis circuit is defined as: $AR = (L - B)/(L + B)$, where L and B denotes the length and width of the beads.

Surface morphology was observed under the scanning electron microscope (SEM) (JEOL, JSM6510LV, USA) at 15 kV. The surface of the dry beads is prepared by removing the top of the thermally sprayed layer of platinum (ion sputter, 30 s). Digital images were collected at magnifications of 50×, 500× and 5000×. The elemental analysis of the cross-sections was done by energy-dispersive X-ray spectroscopy (EDX).

2.6. Water holding capacity

The water content was determined as a measure of the water holding capacity of the beads. The weight of 40–60 randomly selected beads from each batch before and after complete removal of moisture by drying beads was determined on AG 245 wt (Mettler Toledo International) (Das et al., 2011). The water content (WC) was calculated using the following equations: $WC\% = (W_W - W_D)/W_W \times 100\%$, where, W_W and W_D represent the weight of the beads before and after drying, respectively.

2.7. Drug loading and encapsulation efficiency

The beads prepared with different content mesalazine and combination of *pectin-TEOS-4* and *pectin-Ca-TEOS-4*, were immersed in 20–50 mL of phosphate buffer with pH = 6.8. After swelling, the beads were crushed and withstand for a further 24 h. The solution was filtered then and the amount of mesalazine was defined. The loading of mesalazine was defined as the ratio between the weight of mesalazine in the beads and the weight of beads

loaded with mesalazine: Loading of mesalazine (LM) % = Weight of mesalazine/Weight of beads \times 100%. For definition of encapsulation efficiency of mesalazine (%) following formula was used: Encapsulation efficiency (EE) % = Actual amount of mesalazine encapsulated in beads/Theoretical amount of mesalazine used for preparation of beads \times 100%. Mesalazine concentration was determined at a wavelength of 303 nm for a pre-built, depending mesalazine in concentrations ranging from 10 to 100 mg/mL (Moharana, Banerjee, Panda, & Muduli, 2011).

2.8. Evaluation of the stability of beads in an environment simulating the GIT

The stability of the beads were assessed in a solution simulating the GIT. The dry beads of known weight (20 mg) were placed in a glass vial containing 20 mL of the simulated gastric medium (pH 1.09, 0.08 M HCl and 0.03 M NaCl) and incubated at 37 °C for 2 h. After that, the swollen beads were withdrawn, weighed, placed immediately in a glass vial containing 20 mL of the simulated intestinal medium (pH 6.80, 0.05 M KH₂PO₄ and 0.05 M NaOH) and incubated at 37 °C for 8 h or until completely dissolved beads. The beads were periodically withdrawn and weighed. All experiments were done in triplicate.

2.9. Mesalazine release in vitro

To examine the release behavior of mesalazine from beads in GIT *in vitro*, samples (20 mg) were added to 20 mL of the simulated gastric medium (pH 1.09, 0.08 M HCl and 0.03 M NaCl) and were incubated at 37 °C for 2 h; subsequently transferred into 20 mL of the simulated intestinal mediums: pH 6.80 (0.05 M KH₂PO₄ and 0.05 M NaOH) for 6 h and pH 7.40 (0.07 M KH₂PO₄ and 0.07 M NaHPO₄) for 16 h or until completely dissolved beads. At predetermined time intervals, samples of 20 mL were collected from the release medium and replaced by an equal volume of fresh buffer solution. The amount of mesalazine released from the beads was assayed by spectroscopy at 303 nm (Moharana et al., 2011).

3. Results and discussion

In this work, commercial apple pectins AU701 and AU202 with different degree of methylation were used. Both pectins are high molecular compounds, containing D-galacturonic acid residues as the main component of macromolecules (Table 1).

3.1. Formation of pectin-silica gels

In preparation of the pectin-silica gels, TEOS was applied as silicon source; mineral acid was used as the catalyst, which leads to increasing reaction speed and to reducing time of gel maturation to 24 h. The preparation of silica gels by the sol-gel method starts from TEOS in an organic solvent, most often ethanol (Pierre & Rigacci, 2011; Vaskevich, Gaishun, Kovalenko, & Sidsky, 2011). In order to eliminate the influence of ethanol in the gelling reaction and to determine the interaction of pectin and silica, pectin-silica gels were obtained in the absence of ethanol. In the preparation of pectin-silica gels in the form of plates, 2% solutions of LM and HM pectins, different amounts of TEOS were used. The introduction of TEOS and a small amount of HCl as catalyst induced the gelation of AU701 solutions, at concentration of TEOS beginning from 0.25 M. As a result, the pectin-silica gels with different mechanical properties were obtained (Table 2). The experiment with AU202 revealed that the gelation of the HM pectin solutions proceeds with difficulty at low TEOS concentrations (0.25 and 0.5 M), viscous liquid is formed. However, using TEOS concentrations of 0.75 M and 1.00 M, the gels are formed (Table 2).

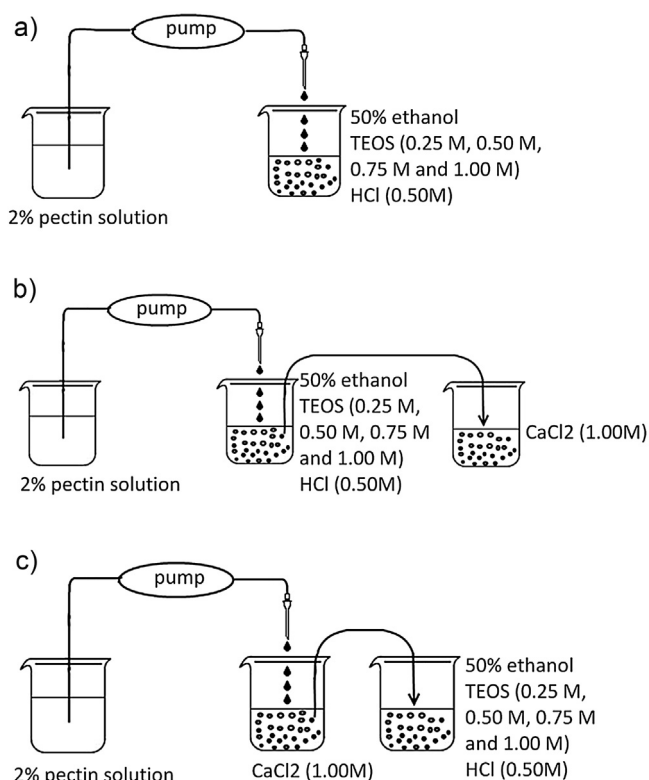


Fig. 1. Preparation of pectin-TEOS (a), pectin-TEOS-Ca (b), pectin-Ca-TEOS (c) beads.

Therefore, during the preparation of pectin-silica gels in a form of plates were shown the chemical interaction of the pectins with TEOS is occurring without addition of ethanol in the reaction mixture. The modification of hydroxypropylcellulose and carboxymethylcellulose by TEOS have shown also occurs without ethanol (Angelova et al., 2012; Rangelova et al., 2014). However, the using ethanol during the preparation of pectin-silica gels in the form of beads is necessary. If the synthesis of pectin-silica beads carries out without ethanol, the pectin will dissolve in the reaction system earlier than they entered into a chemical reaction with TEOS. It should be noted that acetone or other polar solvents could be used instead of ethanol.

For preparation the pectin-silica beads pectin AU701, which forms strong gels in a wide range of TEOS concentrations (Table 2), was used. Beads pectin-TEOS were synthesized by dispersion the pectin solution in TEOS-ethanol-water systems with an acid catalyst (HCl) and subsequent exposure for 24 h (Fig. 1a). Beads pectin-TEOS-Ca (Fig. 1b) were synthesized from pre-formed pectin-TEOS beads by immersing in CaCl₂ solution for 1 h. Beads pectin-Ca-TEOS (Fig. 1c) were synthesized by a two-step procedure: calcium pectinate beads prepared by ionotropic gelation were immersed in TEOS-ethanol-water systems with an acid catalyst (HCl) for 24 h.

The mean diameter of beads ranges from 0.98 to 1.13 mm for the dried samples, and from 2.98 to 3.40 mm for the wet samples. From aspect ratio, it can be seen that almost all the beads were spherical in shape. In most cases (Table 3), bead size and water content were not significant depended on the formulation conditions of the pectin-silica beads (Table 3).

3.2. Infrared spectroscopy pectin-silica gels

The method of FTIR-spectroscopy for establishing chemical bonds in pectin-silica gels was used. Fig. 2a shows the FTIR spectrum of pectin AU701, which has following absorption bands: at

Table 3
The formulation composition, size and water holding capacity of the beads.

Beads	C (TЭOC) mol/l	C (CaCl ₂) mol/l	Wet beads		Dry beads		WC (%)
			Size (mm ± SD)	AR	Size (mm ± SD)	AR	
<i>pectin-TEOS-1</i>	0.25	–	3.12 ± 0.12	0.03	0.99 ± 0.10	0.05	96.8 ± 0.2
<i>pectin-TEOS-2</i>	0.50	–	3.14 ± 0.22	0.03	0.98 ± 0.09	0.06	96.1 ± 0.3
<i>pectin-TEOS-3</i>	0.75	–	3.21 ± 0.18	0.03	0.98 ± 0.08	0.06	96.7 ± 1.6
<i>pectin-TEOS-4</i>	1.00	–	3.07 ± 0.10	0.03	0.98 ± 0.10	0.06	95.1 ± 1.4
<i>pectin-TEOS-Ca-1</i>	0.25	1.00	3.40 ± 0.16	0.03	1.01 ± 0.14	0.06	95.6 ± 0.7
<i>pectin-TEOS-Ca-2</i>	0.50	1.00	3.00 ± 0.17	0.04	0.95 ± 0.11	0.06	96.0 ± 0.2
<i>pectin-TEOS-Ca-3</i>	0.75	1.00	3.07 ± 0.22	0.04	1.16 ± 0.10	0.03	96.3 ± 0.4
<i>pectin-TEOS-Ca-4</i>	1.00	1.00	3.12 ± 0.08	0.02	1.05 ± 0.13	0.03	95.4 ± 0.4
<i>pectin-Ca-TEOS-1</i>	0.25	1.00	3.03 ± 0.20	0.04	0.97 ± 0.08	0.09	96.9 ± 0.2
<i>pectin-Ca-TEOS-2</i>	0.50	1.00	3.08 ± 0.16	0.04	0.97 ± 0.14	0.09	95.5 ± 0.5
<i>pectin-Ca-TEOS-3</i>	0.75	1.00	3.17 ± 0.10	0.03	0.98 ± 0.07	0.08	94.8 ± 0.1
<i>pectin-Ca-TEOS-4</i>	1.00	1.00	3.04 ± 0.09	0.03	1.04 ± 0.13	0.05	93.8 ± 0.2
<i>Ca-pectin</i>	–	1.00	2.98 ± 0.14	0.02	1.04 ± 0.09	0.03	95.8 ± 0.2

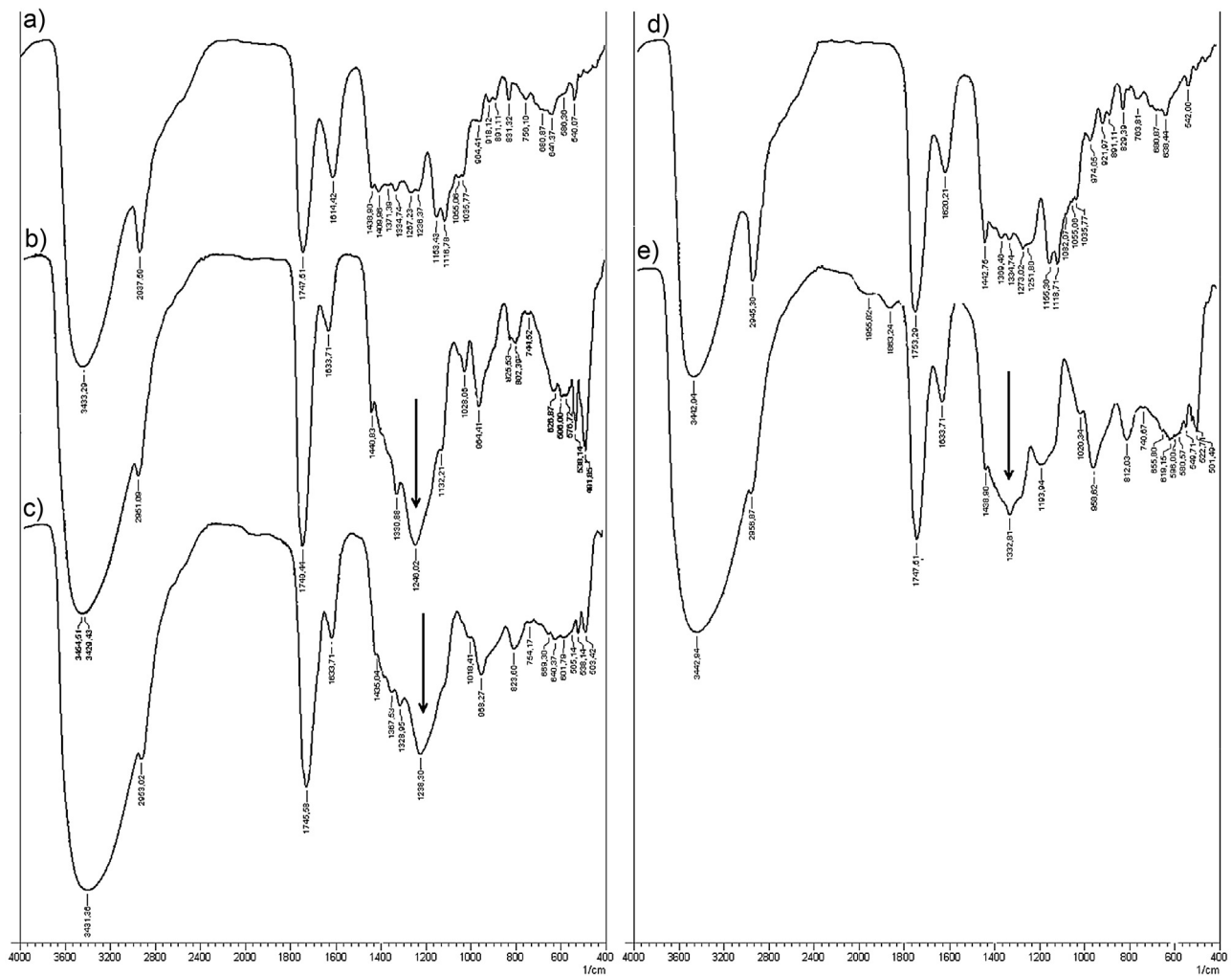


Fig. 2. FTIR spectra of *pectin AU701* (a), *AU701-4* plate (b), *pectin-TEOS-4* bead (c), *pectin AU202* (d), *AU202-4* plate (e).

3433 cm^{-1} corresponds to the stretching vibrations of hydroxyl groups, at 2938 cm^{-1} corresponds to stretching vibrations of the methyl esters groups or C–H bonds of pyranoid ring carbons (Calce, Bugatti, Vittoria, & De Luca, 2012; Lim, Yoo, Ko, & Lee, 2012; Synytsya, Copřakova, Matejka, & Machovic, 2003), at 1748 cm^{-1} corresponds to stretching vibrations of carboxyl groups (Ismail, Ramli, Hani, & Meon, 2012; Synytsya et al., 2003), at 1614 cm^{-1} corresponds to stretching vibrations of the carbonyl moieties in carboxyl

and methyl ester groups (Copikova, Synytsya, Cerna, Kaasova, & Novotna, 2001). The region of $1440\text{--}1237\text{ cm}^{-1}$ are occupied by asymmetric stretching vibrations of the –C–O–C– bonds and –CH groups or stretching vibration of methyl esters groups (Copikova et al., 2001; Synytsya et al., 2003). The region of $1200\text{--}1000\text{ cm}^{-1}$ corresponds to skeletal C–O and C–C vibration bands of glycosidic bonds and a pyranoid ring, and is considered to be the “fingerprint” region that is specific to polysaccharides (Synytsya et al., 2003). The

1153–1117 cm^{-1} region contains the asymmetric stretching fluctuations of $-\text{C}-\text{O}-\text{C}-$ and $-\text{C}-\text{C}$ bonds (Copikova et al., 2001; Kundu, Sarmah, & Sarkar, 1995; Kamnev, Calce, Tarantilis, Tugarova, & De Luca, 2015; Synytsya et al., 2003), the 1055–1036 cm^{-1} region corresponds to the symmetric stretching vibrations of $-\text{C}-\text{O}-\text{C}-$ and $-\text{C}-\text{C}$ bonds (Copikova et al., 2001; Synytsya et al., 2003). The region of 964–891 cm^{-1} contains the deformation vibrations of the $-\text{C}-\text{OH}$ groups (Copikova et al., 2001; Synytsya et al., 2003). The bands at 831, 640 and 540 cm^{-1} correspond to bending vibrations of the $-\text{C}-\text{OH}$ and $-\text{C}-\text{H}$ groups (Copikova et al., 2001; Synytsya et al., 2003).

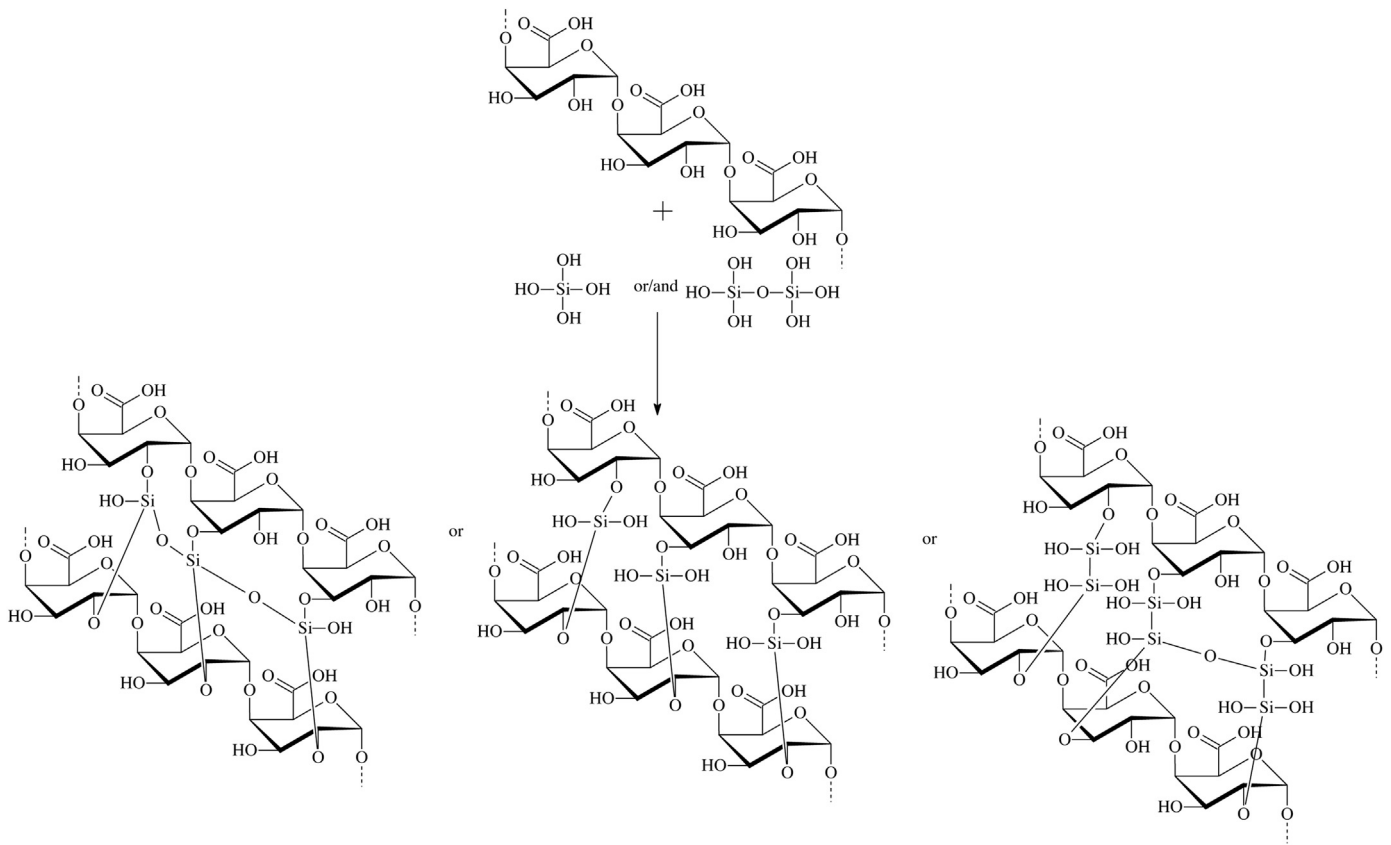
In the FTIR spectrum of pectin-silica plate AU701-4 (Fig. 2b), the following absorption bands are observed: an increasing signal intensity in region of 3455–3429 cm^{-1} corresponds to the imposition of the stretching vibrations of $-\text{C}-\text{OH}$ and $-\text{Si}-\text{OH}$ groups, the region of 2951 cm^{-1} contains the stretching vibrations of the $\text{C}-\text{H}$ bonds of a pyranoid ring, at 1749 cm^{-1} corresponds to stretching vibrations of the carboxyl groups, at 1634 cm^{-1} stretching vibrations of the carbonyl moieties in the carboxyl group is saved, in the region of 1440–1330 cm^{-1} asymmetric stretching vibrations of the $-\text{C}-\text{O}-\text{C}-$ groups or stretching vibrations methyl ester groups is also saved. In the field of 1246 cm^{-1} vibrations of $-\text{C}-\text{O}-\text{Si}-$ groups appear which absent in the spectrum of native pectin. In region of 1132 cm^{-1} and 802 cm^{-1} vibrations of $-\text{Si}-\text{O}-\text{Si}-$ and $-\text{C}-\text{O}-\text{Si}-$ groups appear (Gendron-Badou, Coradin, Maquet, Frohlich, & Livage, 2003; Han, Taylor, Mantle, & Knowles, 2007; Kim et al., 2009; Nenkova, Radev, Rangelova, Aleksiev, & Samuneva, 2007; Swann & Patwardhan, 2011), which also absent in the spectrum of native pectin. The region of 1028 cm^{-1} corresponds to the symmetric stretching vibrations of $-\text{C}-\text{O}-\text{C}-$ groups, increasing signal intensity in the region of 964 cm^{-1} indicates the occurrence of symmetric stretching vibrations of $\text{Si}-\text{OH}$ groups, which are superimposed with bending vibrations of $-\text{C}-\text{OH}$ groups. The absence of bands at 891 cm^{-1} corresponded to $-\text{C}-\text{OH}$ groups is evidence of their partial replacement by $-\text{C}-\text{O}-\text{Si}-$ bonds. The signal intensity in the region of 627–576 cm^{-1} corresponds to deformation vibrations of $-\text{C}-\text{H}$ groups. The deformation vibrations of $-\text{Si}-\text{O}-\text{Si}-$ bonds appear at 492 cm^{-1} , which absent in spectrum of native pectin. The absence of bands at 720 cm^{-1} and 645 cm^{-1} is an indication that the precursor used to obtain the silica was completely hydrolyzed (Toki, Chow, Ohnaka, Samura, & Saegusa, 1992; Vinogradova, Estrada, & Moreno, 2006). Fig. 2b and c shows that the absorption bands in FTIR spectra of pectin-TEOS-4 beads and AU701-4 plate are identical to each other.

In the FTIR spectrum of pectin AU202 (Fig. 2d), the absorption bands are identical to the absorption bands of pectin AU701. The exceptions are signals at 2938 cm^{-1} and 1443 cm^{-1} , where more

intense stretching vibrations of the methyl esters groups or $\text{C}-\text{H}$ bonds and methyl groups is observed respectively (Calce et al., 2012; Lim et al., 2012; Synytsya et al., 2003). The FTIR spectrum of AU202-4 plate (Fig. 2e) is similar to the FTIR spectrum of AU701-4 plate. The most intense signals vibrations of $-\text{Si}-\text{O}-\text{Si}-$ bonds that absent in the FTIR spectra of original pectins appear at 1246 cm^{-1} and 1332 cm^{-1} . The stretching vibrations of the methyl esters at 1438 cm^{-1} are saved.

The FTIR spectra of biogenic silica (Gendron-Badou et al., 2003; Swann & Patwardhan, 2011), synthesized polysaccharide-silica materials (Agoudjil et al., 2012; Angelova et al., 2012; Assifaoui et al., 2013; Chernev, Todorova, Djambazov, Salvado, & Ivanova, 2014; Nurdin & Purwasasmita, 2013; Rangelova et al., 2014; Samuneva et al., 2008;), as well of the produced pectin-silica gels have absorption bands in the 1150–1000 cm^{-1} and 490–450 cm^{-1} regions, corresponding to $-\text{Si}-\text{O}-\text{Si}-$ bonds. The absorption bands in the region of 970–950 cm^{-1} correspond to $-\text{Si}-\text{OH}$ groups. The literature data of FTIR spectroscopy indicate on formation of hydrogen bonds between organic and inorganic components in the pectin-silicate gels. Besides, in the FTIR spectra of AU701-4, pectin-TEOS-4 and AU202-4 gels (Fig. 2), absorption bands at 1246 cm^{-1} and 802 cm^{-1} were identified, which are probably responsible for the formation of bonds $-\text{C}-\text{O}-\text{Si}$ in the synthesized pectin-silica gels. A review of the literature allows us to conclude that the availability an intense absorption band at 1230–1270 cm^{-1} of FTIR spectra indicates the substitution of polysaccharide hydroxyl groups with the formation of covalent bonds. For example, partial acetylation of hydroxyl groups in pectin is the cause of the appearance of absorption bands at 1250 cm^{-1} of $-\text{C}-\text{O}-\text{C}$ bonds (Synytsya et al., 2003). In FTIR spectra of sulfated or phosphate polysaccharides has clearly shown that the absorption bands at 1230–1270 cm^{-1} and 800–850 cm^{-1} appear only after modifications, and indicate the formation of $-\text{C}-\text{O}-\text{S/P}$ bonds (Fan et al., 2011; Huang, Du, Yang, & Fan, 2003; Jung, Bae, Lee, & Jung, 2011; Lin et al., 2007; Suflet, Chitanu, & Popa, 2006; Wang, Zhang, Yao, Zhao, & Qi, 2013). In particular, it was shown on example of sulfated pectins (Bae et al., 2009; Vityazev et al., 2010). Based on the results, we can conclude that, the synthesized pectin-silica gels (AU701-4, pectin-TEOS-4, AU202-4) are formed as a result of chemical interaction between pectin and silica and formation not only hydrogen bonds, but also covalent bonds.

Thus it can be assumed that during the preparation of pectin-silica complexes by using TEOS as silica source, interacts with residues of galacturonic acid, linking them to the second and third hydroxyl, and forming a bridge ($-\text{O}-\text{Si}(\text{OH})_2-\text{O}-$). The reaction can be expressed as follows:



3.3. Structural and mechanical properties of pectin-silica gels

The hydrogels based on pectin AU701 were shown to differ in the silica concentration that leads to differences in the textural parameters (Table 2). Mechanical properties of the pectin-silica gels were determined by uniaxial compression. The profiles of penetration experiments performed on the plates are shown in Fig. 3. Some mechanical parameters were extrapolated from these curves: the

Young modulus (E), obtained from the initial slope of the stress-strain curve at 4% of strain (Table 2); the system hardness, i.e. the maximum positive force registered while attaining the imposed deformation (F_{\max}) (Figs. 3 and 4 a).

The Young modulus of a body is a fundamental property that directly related to its intermolecular binding energy and its structure. It is commonly determined by methods such as compressive testing or indentation testing (Roylance, 2008). The Young modulus

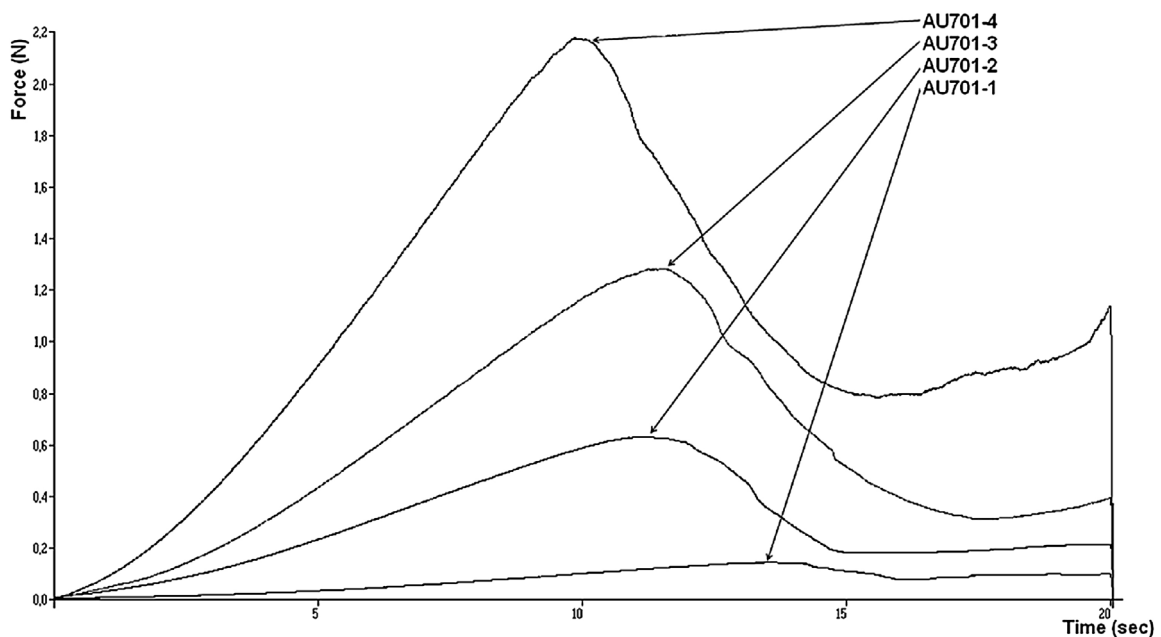


Fig. 3. Texture analysis. Stress-strain curves of AU701-1, AU701-2, AU701-3, AU701-4 plates.

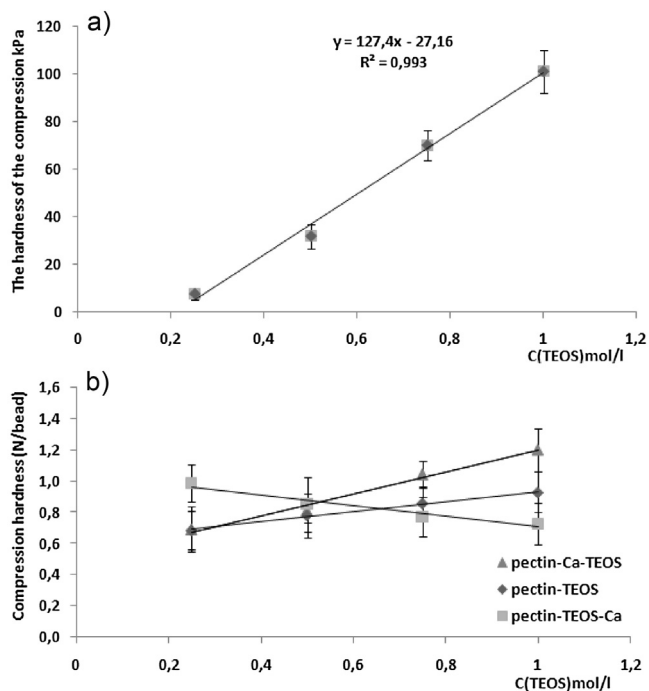


Fig. 4. TEOS concentration dependence of hardness (50% of deformation) of AU701 pectin-silica plates (a) and *pectin-TEOS*, *pectin-TEOS-Ca* and *pectin-Ca-TEOS* beads (b).

is obtained from the load displacement slope of the unloading curve, which is related to the elastic recovery of the plates: $E = (F \times L) / (S \times \Delta L)$, where E is the Young modulus (kPa), S is the total displacement probes (m^2), F compressive force (N), L height of the plate (m), the ΔL absolute compression (m). The variation in the Young modulus within samples of AU701-1, AU701-2, AU701-3,

AU701-4 plates is from 15.4 to 109.9 kPa and dependences on the amount of TEOS used for the preparation (Table 2).

Experiments have shown that plates under physical compression withstand unequal mechanical stresses and, destruction of the gel structure occurs at different compression forces, which indicate the hardness of gels (Fig. 3). The results (Fig. 4a) show that the compressive force, in under which the gel structure is destroyed has a linear dependence on the amount of TEOS used for the gel preparation, a correlation coefficient R^2 is 0.993. The destruction of the gel structures occurs at rising compression forces from 7.5 to 100.9 kPa with increasing of TEOS content from 0.25 to 1.00 M. Thus, it is possible to obtain pectin-silica gels with certain hardness by varying TEOS content during the gel preparation.

The hardness of *pectin-TEOS*, *pectin-TEOS-Ca* and *pectin-Ca-TEOS* beads was found has linear dependence of TEOS concentration, a correlation coefficient R^2 is 0.994–0.954. Unlike the hardness of *pectin-Ca-TEOS* beads, the hardness of *pectin-TEOS-Ca* beads is decreased with increasing TEOS concentration (Fig. 4b). The hardness of *pectin-TEOS* beads is slightly grown with increasing TEOS concentration. Under physical compression *Ca-pectin* and *pectin-Ca-TEOS-4* beads have close hardness values, about 1.11–1.20 N/bead at 50% deformation. The *pectin-Ca-TEOS-4* and *pectin-Ca* beads exhibited the best textural properties in terms of hardness. The *pectin-TEOS-Ca-4*, *pectin-Ca-TEOS-1* and *pectin-TEOS-1* beads have the lower hardness values (Fig. 4b).

3.4. Morphological analysis of the beads by SEM

It can be stated that the addition of different cross-linking agents to pectin, as well as the change of operating conditions of gelation affect morphological characteristics of pectin-silica beads. SEM images illustrate the external structure of the dry beads (Fig. 5). Pectin beads combinations: *pectin-TEOS-4*, *pectin-TEOS-Ca-4*, *pectin-Ca-TEOS-4* and *Ca-pectin* have different shape, surface macro-relief and micro-surface. All beads have a satisfactory spher-

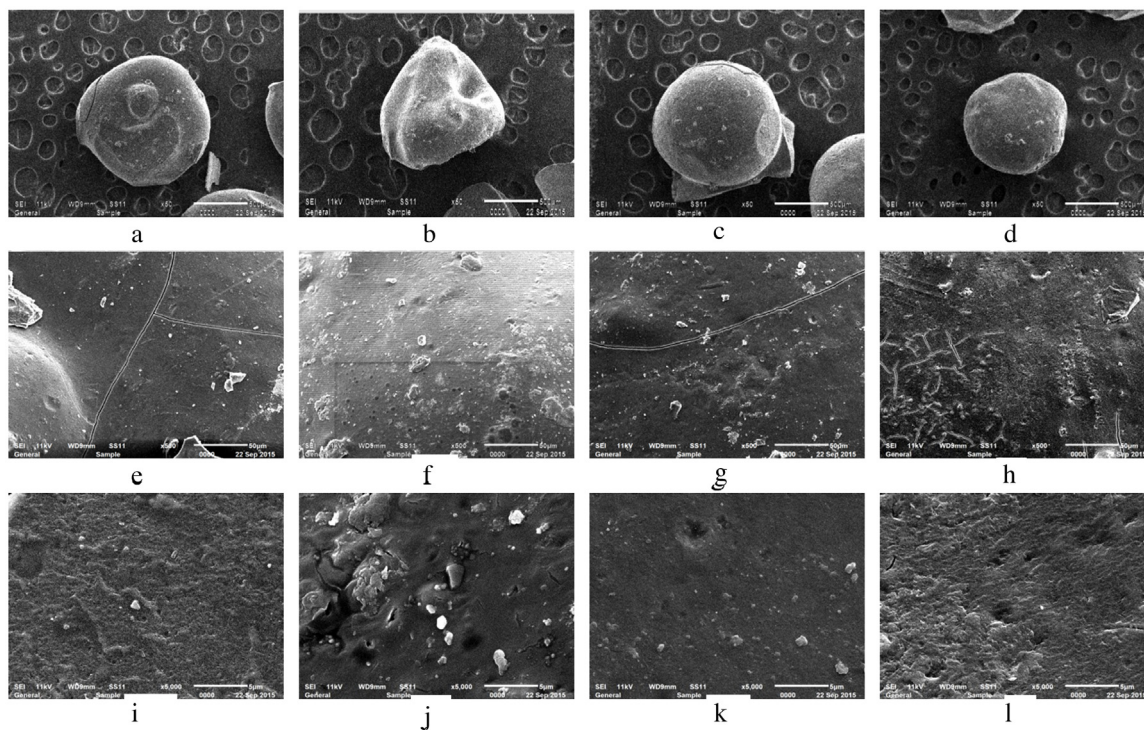


Fig. 5. Scanning electron micrographs of beads: *pectin-TEOS-4* (a), *pectin-TEOS-Ca-4* (b), *pectin-Ca-TEOS-4* (c), *Ca-pectin* (d); magnification 50 \times , scale bar 500 μ m. Microrelief appearances of the beads surfaces: *pectin-TEOS-4* (e), *pectin-TEOS-Ca-4* (f), *pectin-Ca-TEOS-4* (g), *Ca-pectin* (h), magnification 5000 \times , scale bar 5 μ m; and *pectin-TEOS-4* (i), *pectin-TEOS-Ca-4* (j), *pectin-Ca-TEOS-4* (k), *Ca-pectin* (l), magnification 5000 \times , scale bar 5 μ m.

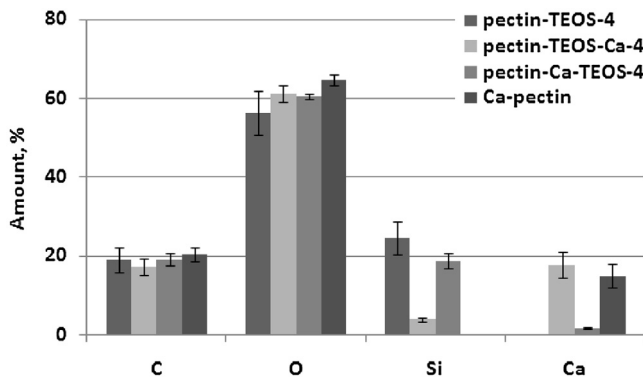


Fig. 6. The elemental composition of the surface layer of beads: *pectin-TEOS-4*, *pectin-TEOS-Ca-4*, *pectin-Ca-TEOS-4*, *Ca-pectin*.

ical shape and a relatively flat surface. The beads *pectin-TEOS* and *Ca-pectin* have a smooth surface microstructure, which is clearly seen in the photographs obtained by increasing the 5000 \times . However, the simultaneous using TEOS and calcium during the preparation of beads *pectin-TEOS-Ca*, *pectin-Ca-TEOS* leads to the formation of a rough and grooved surface. The photographs taken at 500 \times and 5000 \times magnification of samples *pectin-TEOS-Ca-4* and *pectin-Ca-TEOS-4* well reflect the heterogeneity of microrelief. The formation of different sizes grains arranged chaotically is observed. In this case, probably the wet beads (*Ca-pectin* or *pectin-TEOS*) bear partial positive or negative charges accordantly, so direct deposition of silicates or Ca^{2+} is possible, that leads to the formation of granules on the surface of *pectin-TEOS-Ca-4* and *pectin-Ca-TEOS-4* beads. A similar situation was observed in design gelatin–silica hybrid capsules (Coradin & Livage, 2007).

Long cracks formed on the surface of the microrelief were observed in photographs obtained with an increase of 500 \times , of *pectin-TEOS-4* (Fig. 5e) and *pectin-Ca-TEOS-4* (Fig. 5g), which were not noticed in photographs of *pectin-TEOS-Ca-4* (Fig. 5f) and *Ca-pectin* (Fig. 5h). It is possible that the formation of cracks is due to their silicon content of the surface. Elemental analysis made by EDX showed that silicon content of samples *pectin-TEOS-4* and *pectin-Ca-TEOS-4* is higher than 18%. The silicon content of sample *pectin-TEOS-Ca-4* is less than 4%. In addition, the elemental analysis obtained by EDX showed that external layer of the beads is composed of carbon, oxygen and calcium (Fig. 6). The content of carbon and oxygen, remain constant regardless of the bead type ranging from 17% to 20% and from 56% to 65%, respectively. Thus, different content of silicon and calcium in the surface layer depends on the bead making method (Fig. 6).

3.5. Stability of the beads in an environment simulating the GIT

Determining the optimal composition of the pectin–silica gels to mesalazine encapsulation was studied *in vitro* experiments by sequential dissolution of beads in solutions under different pH which simulates the sequence of the beads passage in the human body, i.e., pH initially kept at pH 1.09 (0.08 M HCl and 0.03 M NaCl) for 2 h, then at pH 6.80 (0.02 M NaOH and 0.05 M KH_2PO_4) for 8 h (Fig. 7).

The composition of the surface layer was determined to influence on the strength of beads in the digestive tract. Fig. 7c shows profiles of weight change of *Ca-pectin* and *pectin-TEOS-Ca* beads during sequential incubating in simulated GIT conditions. As seen, pectin *Ca-pectin* and *pectin-TEOS-Ca* beads are stable in an acidic environment. The beads begin to swell in an acidic medium with a pH 1.09 that leads to 8–9 fold increase weight of beads. During subsequent incubation in the medium of phosphate buffer at pH

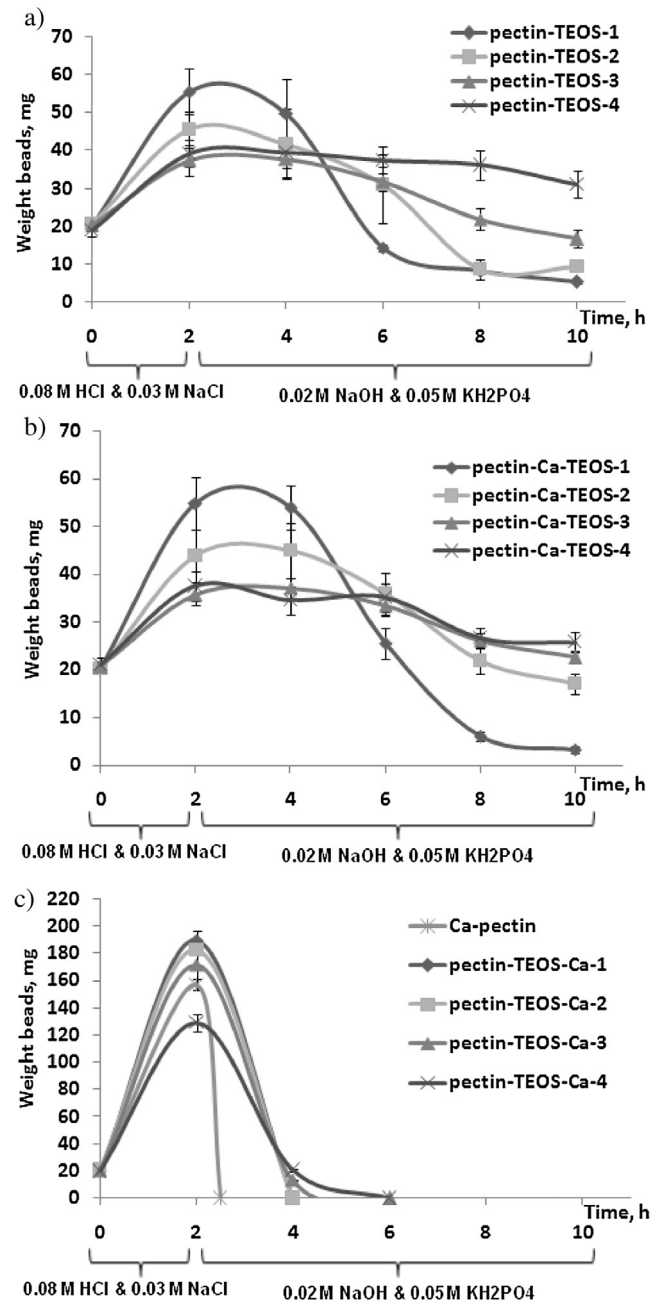


Fig. 7. Profiles of weight change of beads during incubation in simulated GIT conditions. Values are mean \pm s.d. (n = 3).

6.80 was observed reduce the bead weight due to dissolution of calcium pectinate and subsequent bead disintegration. As a result, after 2.5–4.5 h of sequential incubation beads *Ca-pectin* and *pectin-TEOS-Ca* dissolve in simulated intestinal medium (pH 6.80).

The graphs (Fig. 7a and b) have shown the stability of beads *pectin-TEOS* and *pectin-Ca-TEOS* during 8–10 h of sequential incubation in simulated GIT conditions. The beads were stable and swelled in an acidic medium with a pH 1.09, which led to a 2–4 fold increase weight of beads (Fig. 7). During subsequent incubation in the medium of phosphate buffer at pH 6.80 the beads in combination *pectin-TEOS* and *pectin-Ca-TEOS* were stable for 6–8 h. Exceptions are samples *pectin-TEOS-1* and *pectin-Ca-TEOS-1* (minimum TEOS concentration, 0.25 mmol/l), which collapsed almost during 5 h incubation in the medium of phosphate buffer (Fig. 7). Thus, the presence of the silica coating of calcium pectinate and

Table 4
Drug loading and encapsulation efficiency of the beads.

Beads	Initial concentration of mesalazine, %	LM, %	EE, %
<i>pectin-TEOS-1</i>	0.50	4.3	24
<i>pectin-TEOS-2</i>	0.50	3.1	24
<i>pectin-TEOS-3</i>	0.50	2.3	22
<i>pectin-TEOS-4</i>	0.25	1.6	28
	0.50	2.1	23
	1.00	2.9	18
	1.50	4.5	16
	2.00	5.6	16
<i>pectin-Ca-TEOS-1</i>	0.50	3.0	17
<i>pectin-Ca-TEOS-2</i>	0.50	1.6	18
<i>pectin-Ca-TEOS-3</i>	0.50	1.6	16
<i>pectin-Ca-TEOS-4</i>	0.25	0.8	16
	0.50	1.0	14
	1.00	1.9	13
	1.50	3.5	13
	2.00	4.3	10

the silica shell around pectin macromolecule appeared to stabilize significantly the hydrogel network, especially toward dissolution in simulated GIT conditions.

In this regard, beads in combination *pectin-TEOS-Ca*, cannot be considered as a framework for the support of mesalazine, thus, their further research was excluded. Therefore, for the encapsulation of mesalazine should be used beads in combination of *pectin-TEOS* and *pectin-Ca-TEOS*. This approach appears very promising as it allows the association of a soft biocompatible component, pectinate with a tough, non-swelling component, silica.

3.6. Estimation of the mesalazine loading and the encapsulation efficiency of the beads

Effect of the amount of silicon in *pectin-TEOS* and *pectin-Ca-TEOS* beads on the encapsulation efficiency and the drug loading was studied. The pectin-silica beads were prepared from solutions with different contents of TEOS and mesalazine (Table 4). The encapsulation efficiency was found not to change with increasing of silicon content in *pectin-TEOS* and *pectin-Ca-TEOS* beads. The loading of mesalazine is reduced with increasing of silicon content in the beads (Table 4). This happens due to the fact that increasing of silicon content in the beads leads to rising of their weight, while the amount of mesalazine in the beads remains the same (Table 4).

The encapsulation efficiency and loading of mesalazine were revealed to depend on its concentration in the solution from which the beads were prepared. The increase in the concentration of mesalazine in the initial solution leads to the higher values of drug loading. The mesalazine encapsulation efficiency decreases with increasing of the drug concentration from 0.25% to 2.00% in the initial solution. In addition, *pectin-TEOS-4* beads are characterized by the higher encapsulation efficiency than *pectin-Ca-TEOS-4* beads (Table 4). Thus, the optimal concentration of mesalazine in the pectin solution for preparation *pectin-TEOS-4* and *pectin-Ca-TEOS-4* beads is 0.5%. Although some authors use for a bead encapsulation of 1.0% mesalazine solutions, without determination of the concentration-dependent response relationship (Kawadkar et al., 2010).

3.7. In vitro mesalazine release from the beads

Immobilization of mesalazine in *pectin-TEOS-4*, *pectin-Ca-TEOS-4* and *pectin-Ca* beads was performed by the method described in 'Experimental'. Evaluation of the protective effect of the pectin-silica gels in the bead form was provided by *in vitro* experiments of the mesalazine release under pH conditions simulated the

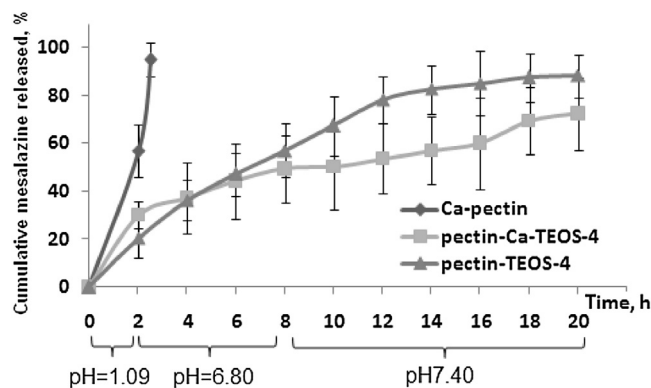


Fig. 8. Mesalazine release profiles of *pectin-TEOS-4*, *pectin-TEOS-Ca-4* and *Ca-pectin* beads under *in vitro* simulated GIT conditions. Values are mean \pm s.d. (n=5).

sequence of the drug passage in the human body, i.e., pH initially kept at 1.09 for 2 h, then at 6.80 for 6 h, and finally at 7.40 for 12 h (Fig. 8). The mesalazine release experiments from *pectin-TEOS-4*, *pectin-Ca-TEOS-4* and *Ca-pectin* beads showed that the type of beads, the nature of the cross-linking agent affects a drug release profile (Fig. 8). The beads *pectin-TEOS-4* and *pectin-Ca-TEOS-4* were shown to release less than 30% of mesalazine during 2 h of incubation in simulated gastric environment, while *Ca-pectin* beads release 57% of the total mesalazine content. The beads *Ca-pectin* are completely dissolved and released 95% of mesalazine during the first 0.5 h of incubation in simulated intestinal medium. The beads *pectin-Ca-TEOS-4* and *pectin-TEOS-4* were shown to disintegrate and release of mesalazine gradually in the simulated intestinal environment. After 2 h of sequential incubation, *pectin-Ca-TEOS-4* beads release about 30% of mesalazine, after 6 h – 44%, after 8 h – 49%, and then each next 2 h the beads release an average of 3% of the total mesalazine content in the beads. After 2 h of sequential incubation, *pectin-TEOS-4* beads release about 20% of mesalazine, after 4 h they release about 36%, after 10 h – 67% of the total mesalazine content in the beads, and then each next 2 h the beads release an average of 4% of mesalazine. Thus, the slope of release curve of *pectin-TEOS-4* beads is steeper in the first 20 h of sequential incubation than that of *pectin-Ca-TEOS-4* beads.

The obtained pectin-silica gels provide a prevention of the drug release of the beads in the stomach and a slow liberation of mesalazine in the intestinal tract that is why the most of mesalazine comes to colon (Fig. 8). Thus, the use pectin-silica gels make it possible controlling mesalazine output in the GIT.

4. Conclusions

A new method for producing pectin-silica gels has been developed. The comparative synthesis of pectin-silica gels by sol-gel gelation of LM and HM pectins with precursor TEOS was obtained. It was shown that synthesis pectin-silica gels can occur in an acidic environment without the use of ethanol. The experiment revealed that the gelation depend on degree of methylation of pectin and TEOS concentration. In the case of LM pectin, monolithic hydrogels were generated through the 24 h starting from minimum concentration of TEOS (0.25 M). Whereas in the case of HM pectin, monolithic hydrogels were produced only at high TEOS concentration (0.75 M).

The FTIR spectra of synthesized pectin-silica gels in presence of ethanol and without it are similar and indicate the formation of hydrogen and covalent bonds between the silica and pectin. The FTIR spectra show intense absorption bands at 1246 cm^{-1} , 1132 cm^{-1} , 802 cm^{-1} , 492 cm^{-1} and 964 cm^{-1} corresponding to the vibrations —C—O—Si— , —Si—O—Si— bonds and —Si—OH groups

accordingly, which are not observed in the FTIR spectra of the native pectins.

The sequential incubation of the beads in simulated gastric fluid for 2 h and in simulated intestinal fluids for 18 h indicates the stability of the pectin-silica beads depending on the gelation technology. In the process of swelling under *in vitro* conditions simulated GIT, the mass of the pectin-silica beads is increased in four times, which is significantly less than the mass increase of ionic gel beads made from pectins and other anionic polysaccharides. The most resistant are beads in combination *pectin-TEOS* and *pectin-Ca-TEOS*. It is shown that the drug release of pectin-silica beads in simulated GIT occurs gradually up to 80% and is directly dependent on the hardness of the beads. It is found that pectin-Ca-TEOS beads are stronger under mechanical compression and its speed of drug release in solutions simulated the intestinal environment is slower than that pectin-TEOS beads.

Therefore, the use of pectin-silica matrices is promising with regard to the development of controlled release of drug formulations. Moreover, the synthesis of pectin-silica matrices can take place in an acidic environment without ethanol, which gives an advantage over other sol-gel methods and opens up new prospects for pectin gels in medicine and biotechnology.

Acknowledgement

The study was partially supported by a grant from the Russian Foundation for Basic Research (14-04-31669).

References

- Agoudjil, N., Sicard, C., Jaouen, V., Garnier, C., Bonnin, E., Steunou, N., et al. (2012). Design and properties of biopolymer-silica hybrid materials: The example of pectin-based biodegradable hydrogels. *Pure and Applied Chemistry*, *84*, 2521–2529.
- Angelova, T., Rangelova, N., Yuryev, R., Georgieva, N., & Muller, R. (2012). Antibacterial activity of SiO₂/hydroxypropyl cellulose hybrid materials containing silver nanoparticles. *Materials Science and Engineering: C*, *32*, 1241–1246.
- Assifaoui, A., Bouyer, F., Chamblin, O., & Cayot, P. (2013). Silica-coated calcium pectinate beads for colonic drug delivery. *Acta Biomaterialia*, *9*, 6218–6225.
- Bae, I. Y., Joe, Y. N., Rha, H. J., Lee, S., Yoo, S. H., & Lee, H. G. (2009). Effect of sulfation on the physicochemical and biological properties of citrus pectins. *Food Hydrocolloids*, *23*, 1980–1983.
- Boonen, A., Dagnelie, P. C., Feleus, A., Hesselink, M. A., Muris, J. W., Stockbrügger, R. W., et al. (2002). The impact of inflammatory bowel disease on labor force participation: Results of a population sampled case-control study. *Inflammatory Bowel Diseases*, *8*(6), 382–389.
- Calce, E., Bugatti, V., Vittoria, V., & De Luca, S. (2012). Solvent-free synthesis of modified pectin compounds promoted by microwave irradiation. *Molecules*, *17*, 12234–12242.
- Capel, F., Nicolai, T., Durand, D., Boulenguer, P., & Langendorff, V. (2006). Calcium and acid induced gelation of (amidated) low methoxyl pectin. *Food Hydrocolloids*, *20*(6), 901–907.
- Chernev, G., Todorova, E., Djambazov, S., Salvado, I. M. M., & Ivanova, J. (2014). Synthesis and structure of sol-gel silica-polysaccharide hybrids. *Journal of Chemical Technology and Metallurgy*, *49*, 128–132.
- Copikova, J., Sinytsya, A., Cerna, M., Kaasova, J., & Novotna, M. (2001). Application of FT-IR spectroscopy in detection of food hydrocolloids in confectionery jellies and food supplements. *Czech Journal of Food Sciences*, *19*(2), 51–56.
- Coradin, T., & Livage, J. (2007). Aqueous silicates in biological sol-gel applications: New perspectives for old precursors. *Accounts of Chemical Research*, *40*, 819–826.
- Das, S., Ng, K.-Y., & Ho, P. C. (2011). Design of a pectin-based microparticle formulation using zinc ions as the cross-linking agent and glutaraldehyde as the hardening agent for colonic-specific delivery of resveratrol: *In vitro* and *in vivo* evaluations. *Journal of Drug Targeting*, *19*(6), 446–457.
- Desreumaux, P., & Ghosh, S. (2006). Review article: Mode of action and delivery of 5-aminosalicylic acid—new evidence. *Alimentary Pharmacology and Therapeutics*, *24*, 2–9.
- Fan, L., Jiang, L., Xu, Y., Zhou, Y., Shen, Y., Xie, W., et al. (2011). Synthesis and anticoagulant activity of sodium alginate sulfates. *Carbohydrate Polymers*, *83*, 1797–1803.
- Gendron-Badou, A., Coradin, T., Maquet, J., Froehlich, F., & Livage, J. (2003). Spectroscopic characterization of biogenic silica. *Journal of Non-Crystalline Solids*, *316*, 331–337.
- Han, Y. H., Taylor, A., Mantle, M., & Knowles, K. (2007). Sol-gel-derived organic-inorganic hybrid materials. *Journal of Non-Crystalline Solids*, *353*, 313–320.
- Huang, R., Du, Y., Yang, J., & Fan, L. (2003). Influence of functional groups on the *in vitro* anticoagulant activity of chitosan sulfate. *Carbohydrate Research*, *338*, 483–489.
- Iacucci, M., de Silva, S., & Ghosh, S. (2010). Mesalazine in inflammatory bowel disease: A trendy topic once again? *Canadian Journal of Gastroenterology*, *24*(2), 127–133.
- Ismail, N. S. M., Ramli, N., Hani, N. M., & Meon, Z. (2012). Extraction and characterization of pectin from dragon fruit (*Hylocereus polyrhizus*) using various extraction conditions. *Sains Malaysiana*, *41*(1), 41–45.
- Jung, H. Y., Bae, I. Y., Lee, S., & Jung, H. G. (2011). Effect of the degree of sulfation on the physicochemical and biological properties of *Pleurotus eryngii* polysaccharides. *Food Hydrocolloids*, *25*, 1291–1295.
- Kamnev, A. A., Calce, E., Tarantilis, P. A., Tugarova, A. V., & De Luca, S. (2015). Pectin functionalised by fatty acids: Diffuse reflectance infrared Fourier transform (DRIFT) spectroscopic characterization. *Journal of Molecular Structure*, *1079*, 74–77.
- Kappelman, M. D., Rifas-Shiman, S. L., Porter, C. Q., Ollendorf, D. A., Sandler, R. S., Galanko, J. A., et al. (2008). Direct health care costs of Crohn's disease and ulcerative colitis in US children and adults. *Gastroenterology*, *135*, 1907–1913.
- Kawadkar, J., Chauhan Meenakshi, K., & Ram, A. (2010). Evaluation of potential of Zn-pectinate gel (ZPG) microparticles containing mesalazine for colonic drug delivery. *Daru*, *18*, 211–220.
- Khasina, E. I., Sgrebneva, M. N., Ovodova, R. G., Golovchenko, V. V., & Ovodov, Y. S. (2003). Gastroprotective effect of lemmann, a pectic polysaccharide from Lemna minor L. *Doklady Biological Sciences*, *390*, 204–206.
- Kim, J. M., Chang, S. M., Kong, S. M., Kim, K.-S., Kim, J. S., & Kim, W.-S. (2009). Control of hydroxyl group content in silica particle synthesized by the sol-precipitation process. *Ceramics International*, *35*, 1015–1019.
- Kornbluth, A., & Sachar, D. B. (2010). Ulcerative colitis practice guidelines in adults: American College of Gastroenterology, Practice Parameters Committee. *The American Journal of Gastroenterology*, *105*, 501–523.
- Kundu, P. K., Sarmah, R., & Sarkar, C. R. (1995). Physico-chemical nature of ramie at different stages of growth. *Indian Journal of Fibre & Textile Research*, *20*, 165–167.
- Latella, G., & Papi, C. (2012). Crucial steps in the natural history of inflammatory bowel disease. *World Journal of Gastroenterology*, *29*, 3790–3799.
- Lim, J., Yoo, J., Ko, S., & Lee, S. (2012). Extraction and characterization of pectin from Yuza (*Citrus junos*) pomace: A comparison of conventional-chemical and combined physicoenzymatic extractions. *Food Hydrocolloids*, *29*, 160–165.
- Lin, C. Z., Guan, H. S., Li, H. H., Yu, G. L., Gu, C. H., & Li, G. Q. (2007). The influence of molecular mass of sulfated propylene glycol ester of low-molecular-weight alginate on anticoagulant activities. *European Polymer Journal*, *43*(7), 3009–3015.
- Longobardi, T., Jacobs, P., & Bernstein, C. N. (2004). Utilization of health care resources by individuals with inflammatory bowel disease in the United States: A profile of time since diagnosis. *The American Journal of Gastroenterology*, *99*(4), 650–655.
- Mohanty, S., & Anigrahi, A. K. (2015). Multiparticulate drug delivery system for colon targeting. *Indian Journal of Pharmaceutical Sciences*, *7*, 433–436.
- Moharana, A. K., Banerjee, M., Panda, S., & Muduli, J. N. (2011). Development and validation of uv spectrophotometric method for the determination of mesalazine in bulk and tablet formulation. *International Journal of Pharmacy and Pharmaceutical Science*, *3*(2), 19–21.
- Munkholm, P. (2003). Review article: The incidence and prevalence of colorectal cancer in inflammatory bowel disease. *Aliment Pharmacol Therapy*, *18*, 1–5.
- Nenkova, S., Radev, L., Rangelova, N., Aleksiev, B., & Samuneva, B. (2007). New sol-gel silica hybrids containing pectin and some metal ions. *Physics and Chemistry of Glasses—European Journal of Glass Science and Technology Part B*, *48*, 164–167.
- Nurdin, D., & Purwasasmita, B. S. (2013). Synthesis and characterization of silica microcapsules with active compounds 2% chlorhexidine using sodium alginate and chitosan coating as medicament of root canal infection. *Solids and Structures (SAS)*, *2*, 9–15.
- Ouyang, Q., Tandon, R., Goh, K. L., Ooi, C. J., Ogata, H., & Fiocchi, C. (2005). The emergence of inflammatory bowel disease in the Asian Pacific region. *Current Opinion in Gastroenterology*, *21*(4), 408–413.
- Patova, O. A., Golovchenko, V. V., & Ovodov, Y. S. (2014). Pectic polysaccharides: Structure and properties. *Russian Chemical Bulletin, International Edition*, *63*(9), 1901–1924.
- Pierre, A. C., & Rigacci, A. (2011). SiO₂ aerogels. In M. A. Aegerter, N. Leventis, & M. M. Koebel (Eds.), *Aerogels handbook, advances in sol-gel derived materials and technologies* (pp. 21–45). New York: Springer Science+Business Media, LLC.
- Popov, S. V., Popova, G. Y., Nikolaeva, S. Y., Golovchenko, V. V., & Ovodova, R. G. (2005). Immunostimulating activity of pectic polysaccharide from *Bergenia crasifolia* (L.) Fritsch. *Phytotherapy Research*, *19*, 1052–1056.
- Popov, S. V., & Ovodov, Y. S. (2013). Polypotency of the immunomodulatory effect of pectins. *Biochemistry (Moscow)*, *78*, 823–835.
- Popov, S. V., Ovodova, R. G., Golovchenko, V. V., Khramova, D. S., Markov, P. A., Smirnov, V. V., et al. (2014). Pectic polysaccharides of the fresh plum *Prunus domestica* L. isolated with a simulated gastric fluid and their anti-inflammatory and antioxidant activities. *Food Chemistry*, *143*, 106–113.

- Rangelova, N., Aleksandrov, L., Angelova, T., Georgieva, N., & Muller, R. (2014). Preparation and characterization of SiO₂/CMC/Ag hybrids with antibacterial properties. *Carbohydrate Research*, 101, 1166–1175.
- Roylance, D. (2008). *Mechanical properties of materials*. pp. 128. MIT.
- Salonen, J., Kaukonen, A. M., Hirvonen, J., & Lehto, V. P. (2008). Mesoporous silicon in drug delivery applications. *Journal of Pharmaceutical Sciences*, 97(2), 632–653.
- Samuneva, B., Kabaivanova, L., Chernev, G., Djambaski, P., Kashchieva, E., Emanuilova, E., et al. (2008). Sol–gel synthesis and structure of silica hybrid materials. *Journal of Sol-Gel Science and Technology*, 48, 73–79.
- Satyrova, T. V., & Mikhailova, E. I. (2010). Ulcerative colitis: The modern view of etiology and pathogenesis (literature review). *Problems of Health and Ecology*, 2(24), 7–11.
- Schroeder, K. W. (2002). Role of mesalazine in acute and long-term treatment of ulcerative colitis and its complications. *Scandinavian Journal of Gastroenterology*, 236, 42–47.
- Shchipunov, Y. A., & Karpenko, T. Y. (2004). Hybrid polysaccharide-silica nanocomposites prepared by the sol-gel technique. *Langmuir*, 20, 3882–3887.
- Sriamornsak, P. (2011). Application of pectin in oral drug delivery. *Expert Opinion on Drug Delivery*, 8(8), 1009–1023.
- Suflet, D. M., Chitanu, G. C., & Popa, V. I. (2006). Phosphorylation of polysaccharides: New results on synthesis and characterisation of phosphorylated cellulose. *Reactive and Functional Polymers*, 66, 1240–1249.
- Swann, G. E. A., & Patwardhan, S. V. (2011). Application of Fourier Transform Infrared Spectroscopy (FTIR) for assessing biogenic silica sample purity in geochemical analyses and palaeoenvironmental research. *Climate of the Past*, 7, 65–74.
- Synytysya, A., Copăková, J., Matejka, P., & Machovic, V. (2003). Fourier Transform Raman and infrared spectroscopy of pectins. *Carbohydrate Research*, 54, 97–106.
- Toki, M., Chow, T., Ohnaka, T., Samura, H., & Saegusa, T. (1992). Structure of poly(vinylpyrrolidone)-silica hybrid. *Polymer Bulletin*, 29, 653–660.
- Usov, A. I., Bilan, M. I., & Klochkova, N. G. (1995). Polysaccharides of algae. 48. Polysaccharide composition of several calcareous red algae: Isolation of alginate from *Corallina pilulifera* P. et R. (Rhodophyta, Corallinaceae). *Botanica Marina*, 38, 43–51.
- Vaskevich, V. V., Gaishun, V. E., Kovalenko, D. L., & Sidsky, V. V. (2011). Protective sol-gel coating with hydrophobic properties, problems of physics. *Mathematics and Technics (in Russian)*, 3(8), 15–19.
- Ventura, I., Jammal, J., & Bianco-Peled, H. (2013). Insights into the nanostructure of low-methoxyl pectin-calcium gels. *Carbohydrate Polymers*, 97, 650–658.
- Vinogradova, E., Estrada, M., & Moreno, A. (2006). Colloidal aggregation phenomena: Spatial structuring of TEOS-derived silica aerogels. *Journal of Colloid and Interface Science*, 298, 209–212.
- Vityazev, F. V., Golovchenko, V. V., Patova, O. A., Drodz, N. N., Makarov, V. A., Shashkov, A. S., et al. (2010). Synthesis of sulfated pectins and their anticoagulant activity. *Biochemistry (Moscow)*, 75, 759–768.
- Vivero-Escoto, J. L., Slowing, I. I., Trewyn, B. G., & Lin, V. S. (2010). Mesoporous silica nanoparticles for intracellular controlled drug delivery. *Small*, 6(18), 1952–1967.
- Wang, X., Zhang, Z., Yao, Q., Zhao, M., & Qi, H. (2013). Phosphorylation of low-molecular-weight polysaccharide from *Enteromorpha linza* with antioxidant activity. *Carbohydrate Polymers*, 96, 371–375.
- Wood, P. J., & Siddiqui, I. R. (1971). Determination of methanol and its application to measurement of pectin ester content and pectin methyl esterase activity. *Analytical Biochemistry*, 39, 418–428.
- Wu, C., Fan, W., Gelinsky, M., Xiao, Y., Chang, J., Friis, T., et al. (2011). In situ repair and protein delivery of silicate-alginate composite microspheres with core-shell structure. *Journal of the Royal Society Interface*, 8, 1804–1814.